Available online at www.sciencedirect.com
ScienceDirect
C. R. Physique 10 (2009) 919–926
COMPTES RENDUS PHYSIQUE

Slow-light: Fascinating physics or potential applications?

Electromagnetically-induced transparency, slow light, and negative group velocities in a room temperature vapor of ^{4}He*

F. Goldfarb [a,*], T. Lauprêtre [a], J. Ruggiero [a], F. Bretenaker [a], J. Ghosh [b,1], R. Ghosh [b]

[a] *Laboratoire Aimé-Cotton, CNRS – Université Paris Sud 11, 91405 Orsay cedex, France*
[b] *School of Physical Sciences, Jawaharlal Nehru University, New Delhi 110067, India*

Available online 30 December 2009

Abstract

^{4}He* at room temperature is a particularly interesting system as velocity changing collisions (VCCs) are necessary to observe ultra-narrow (less than 10 kHz) EIT windows for purely electronic spins in the presence of Doppler broadening. Such narrow resonances are known to be linked to a dramatic reduction of the group velocity of a probe pulse, although the medium is transparent. The evolution of the delay is recorded with respect to the coupling beam intensity and to small Raman detunings. We also demonstrate that it is possible to use optically detuned resonances (*Fano-like profiles*) to see a transition from slow light to negative group velocity. All these measurements are found to be in good agreement with a simple model based on an effective homogeneous linewidth. ***To cite this article: F. Goldfarb et al., C. R. Physique 10 (2009).***

Résumé

Transparence électromagnétiquement induite, lumière lente et vitesses de groupe négatives dans une vapeur de ^{4}He* à température ambiante. L'utilisation d'un gaz d'hélium métastable à température ambiante présente un intérêt particulier du fait du rôle des collisions à changement de vitesse. Celles-ci sont nécessaires pour observer des fenêtres EIT très étroites (moins de 10 kHz) dans ce système élargi par effet Doppler et constitué d'états de spins électroniques. Il est bien connu que, bien que le milieu soit alors transparent, la présence de telles résonances est liée à une forte réduction de la vitesse de groupe d'une impulsion sonde. Nous avons observé l'évolution du délai avec l'intensité du laser de pompe et de petits désaccords Raman. Nous avons également montré qu'il était possible d'utiliser des résonances en présence de désaccord optique (profils de Fano) pour observer la transition d'un régime de lumière lente à des vitesses de groupe négatives. Toutes ces mesures sont en bon accord avec un modèle simple utilisant une largeur homogène effective. ***Pour citer cet article : F. Goldfarb et al., C. R. Physique 10 (2009).***

Keywords: Metastable helium; EIT; Slow light; Fast light; Fano profiles

Mots-clés : Hélium métastable ; EIT ; Lumière lente ; Lumière rapide ; Profils de Fano

* Corresponding author.
E-mail address: fabienne.goldfarb@u-psud.fr (F. Goldfarb).
[1] Present address: ICFO – Institut de Ciencies Fotoniques, Mediterranean Technology Park, 08860 Castelldefels (Barcelona), Spain.

1631-0705/$ – see front matter
doi:10.1016/j.crhy.2009.10.004

1. Introduction

Electromagnetically induced transparency (EIT) in three-level Λ-systems is based on quantum interference effects involving coherence between the two lower states [1,2]. Such sharp EIT resonances are known to be coupled to a dramatic reduction of the group velocity of the probe [3]. The efficiency of EIT is strongly dependent on the lifetime of this Raman coherence and the narrowest features and lowest group velocities in gases were obtained with cold atoms [4]. However, Doppler broadened gases can also exhibit quite steep resonances [5] and the capability to delay a pulse of light in a simple room-temperature system in a tunable and controllable fashion opens the door to possible applications.

It was already demonstrated that metastable ^{4}He* is an ideal candidate for ultra-narrow EIT in a system involving only electronic spins in a vapor at room temperature [6]. The physics of the system cannot be understood without considering the favorable role played by velocity changing collisions (VCCs) through four different effects involving the peculiarities of He*: (i) as they experience many VCCs, atoms jump from one velocity class to another, permitting optical pumping of a large part of the Doppler profile even with a few milliwatts of coupling power; (ii) because of collisions, the transit of the atoms into the laser beam is diffusive and not ballistic, which helps to increase the Raman coherence lifetime; (iii) this is possible because collisions involving He atoms in the zero spin and angular momentum ground state do not depolarize the colliding He*; and (iv) Penning ionization among identically polarized He* atoms is almost forbidden [7]. These specific properties were studied and notably used for He* Bose–Einstein condensation [8,9].

EIT resonances as narrow as a few kHz were recorded and group velocities lower than 7000 m s^{-1} could be seen with our set-up. A theoretical model which takes into account the effects of collisions and the influx of atoms into the beam allowed us to simulate our data quite well and showed that the effects of decoherence and finite transit time into the beam should be separately considered for a correct modelling of the phenomena [10].

In this article, we show that the inhomogeneous Doppler broadening can be simply included in a calculation valid for homogeneously broadened media through an effective spectral width, which represents the part of atoms that are pumped into one Zeeman sublevel and can thus participate in the EIT phenomena. We present experimental results on slow light recorded with small Raman detunings, and we show the transition from slow light to negative group velocity light propagation when the coupling beam is out of optical resonance.

2. Experimental set-up

Some years ago, it was proved that it is possible to select a closed Λ-system with polarized light resonant with the $^3S_1 \rightarrow {}^3P_1$ transition of ^{4}He and to use it for achieving sub-recoil cooling via Velocity Selective Coherent Population Trapping (VSCPT) [11] or Coherent Population Trapping (CPT) for magnetometry applications [12]. The relevant level scheme is given in Fig. 1(a). A σ^+ polarized light pumps the atoms in the sublevel $m = -1$, which can be probed by a σ^- polarized laser beam. Because the transition between the two Zeeman sublevels of spin projection $m = 0$ is forbidden, the level $^3S_1$, $m = 0$ is emptied after a few pumping cycles. The only relevant sublevels are thus the two ground states $^3S_1$, $m = \pm 1$ and the excited state $^3P_1$, $m = 0$, which yield a very pure Λ-system.

The experimental setup is sketched in Fig. 1(b). Light at 1.083 μm is provided by a diode laser (model SDL-6700). The beam is spatially filtered by a single-mode fiber before being separated by a polarizing beamsplitter into a pump beam and a probe beam. Their frequencies and intensities are controlled by two acousto-optic modulators AO_1 and AO_2. The pump beam is fed continuously at a fixed frequency. The probe beam can be linearly scanned in frequency or modulated in intensity. These two beams are recombined and a quarter-wave plate transforms them into two orthogonal circular polarizations before entering the helium cell. A telescope allows us to adjust the size of the Gaussian beam inside the cell. The results presented here were obtained with a 1 cm beam diameter (at $1/e^2$ of the maximum intensity). Another quarter-wave plate transforms back the coupling and probe beams into two orthogonal linear polarizations, so that the pump laser can be stopped by a polarizer, which allows us to detect only the probe beam. In the following reported experiments, the probe laser power was set around 70 μW.

The helium cell is 2.5 cm long, and is filled with ^{4}He at 1 Torr, which corresponds to an optical coherence decay rate of $\Gamma = 1.4 \times 10^8$ s^{-1} [13]. At room temperature, the Doppler half-width at half-maximum $W_D/2\pi$ is around 0.85 GHz. He atoms are excited to the metastable state by an RF discharge at 27 MHz. At the center of the Doppler profile of the optical transition and for a vanishing light intensity, the cell absorbs about 70% of the incident intensity.

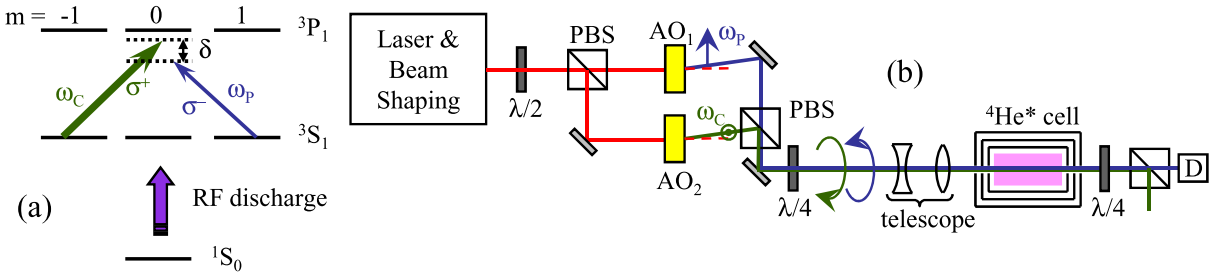

Fig. 1. (a) Relevant level scheme. ω_P and ω_C are the frequencies of the probe and coupling beams, respectively. δ is the Raman detuning: as the two ground levels are degenerate, $\delta = \omega_P - \omega_C$. (b) Experimental setup. PBS: polarization beam splitter; D: detector; AOs: acousto-optic modulators.

These figures of course vary with experimental parameters, such as the RF discharge power. The cell is enclosed in a three-layer mu-metal magnetic shielding.

When the coupling beam frequency ω_C is tuned close to the maximum absorption frequency of the $^3S_1 \rightarrow {}^3P_1$ transition, we probe the EIT window created by this coupling beam by scanning the frequency ω_P of the weak probe beam around ω_C, thus scanning the Raman detuning $\delta/2\pi = (\omega_P - \omega_C)/2\pi$ around 0 at 100 kHz s^{-1}. Delays are measured by recording the shape of a 50 μs Gaussian pulse probe and comparing it to a reference pulse recorded without any discharge inside the cell.

3. EIT and slow light at optical resonance

Figs. 2 and 3 show the results obtained for the resonance widths and group delays at Raman resonance ($\delta = 0$), respectively, when the coupling beam frequency is roughly at the center of the Doppler profile. The inset in Fig. 2 is a typical EIT resonance obtained in this case, together with a Lorentzian fit.

We can model the phenomenon if we introduce an effective spectral width W, which is the width of the spectral distribution of the moving atoms that are pumped into one Zeeman sublevel by the coupling laser and thus experience EIT. It was suggested that in a Doppler broadened gas, the evolution of the EIT window width with respect to the coupling beam intensity is similar to its evolution in an homogeneously broadened medium if all the atoms are pumped into the dark state: the homogeneous width should just be replaced by the Doppler width $W_D/2\pi$ [14]. If the optical pumping is not fully achieved, one can introduce an effective width $W < W_D$, which reflects the fact that only the fraction of the atoms that are pumped into the probed sublevel participates in the EIT.

We call Γ_R the Raman coherence decay rate and Ω_C the coupling beam Rabi frequency, the orders of magnitude of which are respectively $\Gamma_R/2\pi \sim 10^4$–10^5 Hz and $\Omega_C/2\pi \sim 10^6$–10^7 Hz. The response of the system, at first order in the probe Rabi frequency and when the major part of atoms are assumed to be optically pumped, can then be simply calculated by the usual density matrix equations [2][2]:

$$\chi = \frac{Nd^2}{2\varepsilon_0\hbar}\left[\frac{4\delta\Omega_C^2 + i4(\Gamma_R\Omega_C^2 + 2(W+\Gamma)(\Gamma_R^2+\delta^2))}{(2\Gamma_R(2W+\Gamma)+\Omega_C^2)^2 + (2\delta)^2(2W+\Gamma)^2}\right] \tag{1}$$

where we have assumed that δ, $\Gamma_R \ll \Gamma$, Ω_C and the coupling beam is at optical resonance. N is the density of atoms involved in EIT, d the dipole moment of the probed transition, and ε_0 the vacuum permittivity. The EIT resonance width thus obeys a very simple equation derived from the imaginary part of the susceptibility given above:

$$\Gamma_{EIT} = 2\Gamma_R + \frac{\Omega_C^2}{2W+\Gamma} \tag{2}$$

The effective width W reflects the fact that VCCs make atoms jump from one velocity class to another, hence partly spreading optical pumping over the Doppler profile even at relatively low coupling power. In metastable helium, this is possible because of the peculiarities of this atom: the metastable state and the spin polarization are preserved when it experiences velocity changing collisions [6,7].

[2] Our Rabi frequency Ω_C is the real angular frequency of the Rabi oscillations, and is thus double of that defined in Ref. [14].

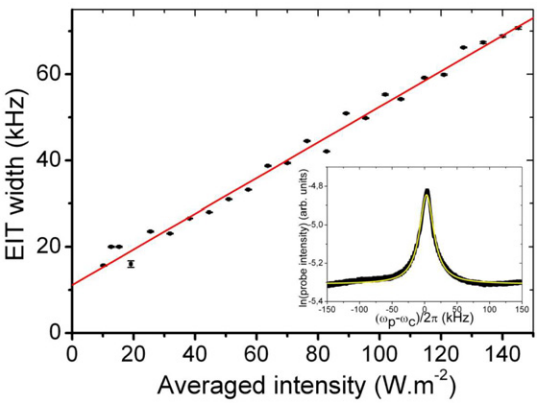

Fig. 2. EIT peak widths are plotted with respect to the averaged intensity (inset: EIT peak for a coupling intensity around 50 W m^{-2}). The 412 Hz/(W m^{-2}) slope is related to the number of atoms involved in the phenomenon, and the 11 kHz measured intercept is twice the Raman coherence decay rate, which is then estimated to be 5.5 kHz.

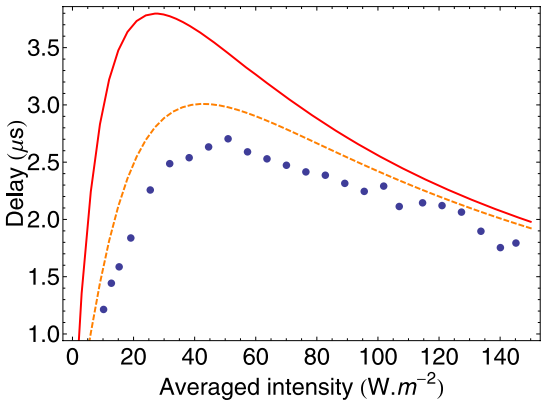

Fig. 3. Recorded delays of a 50 μs width Gaussian pulse for the same coupling intensities. The theoretical curves use the effective width $W/2\pi = 0.42$ GHz and the 5.5 kHz Raman coherence decay rate deduced from Fig. 2. The full red line is given by Eq. (3), and the dashed orange one by Eq. (5) with a Raman detuning $\delta/2\pi = 3.8$ kHz consistent with a small shift of the recorded resonances. (For interpretation of the references to colour in this figure legend, the reader is referred to the web version of this article.)

With our experimental conditions, we found a slope of 412 Hz/(W m^{-2}) and an intercept of 11 kHz, which gives a Raman decay rate Γ_R around $2\pi * 5.5$ kHz. The slope corresponds to a width $W/2\pi$ of 0.42 GHz, which means that the effective width over which atoms are optically pumped and thus participate in EIT is half of the Doppler width.[3]

We can then check the validity of the approximation for the delay values recorded as a function of the coupling intensity as given in Fig. 3. If we use the same approximations as before, the evolution of the group delay at Raman resonance with respect to the coupling Rabi frequency should be given by the following equation:

$$\tau_g = \frac{L}{2c}\left(\Re e(\chi) + \omega_0 \frac{d\Re e(\chi)}{d\delta}\right)\Big|_{\delta=0} = -\ln(T_0)\frac{(2W+\Gamma)\Omega_C^2}{[2\Gamma_R(2W+\Gamma)+\Omega_C^2]^2} \tag{3}$$

where L is the length of the cell, c the speed of light in vacuum, ω_0 the frequency of the optical transition and T_0 the transmission of the cell without the coupling beam. T_0 is given by

$$\ln(T_0) = -L\frac{Nd^2\omega_0}{\epsilon_0\hbar c(2W+\Gamma)}$$

The maximum value $-\ln(T_0)/8\Gamma_R$ for the delay given by expression (3) is much higher than the experimental value plotted in Fig. 3. The direct measurement of a 30% transmission with a faint probe laser gives a maximum delay around 4 μs, while the maximum experimental value is around 2.8 μs. A possible explanation would be that the data were recorded with a small Raman detuning, which was indeed visible on the EIT resonances. As it is explained below, it is possible to derive a theoretical equation with a small Raman detuning, which gives an adequate match as plotted in Fig. 3.

Using the same hypothesis as before, the transmission at resonance can be derived from $\Im m(\chi)$ using Eq. (1):

$$\ln(T) = \frac{\ln(T_0)}{1+\frac{\Omega_C^2}{2\Gamma_R(2W+\Gamma)}} \tag{4}$$

The measured transmission and the theoretical curve deduced from this equation with the same parameter values as before are plotted in Fig. 4. The experimental points are below the calculated ones. It was already the case for our first

[3] In Ref. [6], it was found that the effective width was the Doppler width because of a mistake in the transition strength used for calculating the Rabi frequency, which was taken at 0.54 instead of 0.27.

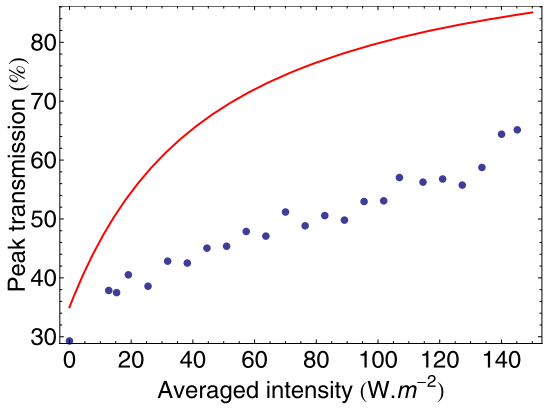

Fig. 4. Measured evolution of the EIT peak transmission versus coupling beam intensity. The theoretical plot is obtained with Eq. (4), keeping the parameters deduced previously from Figs. 2 and 3.

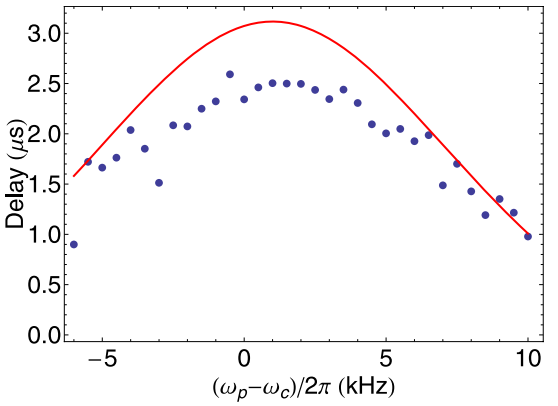

Fig. 5. Delays measured for a 45 W m^{-2} coupling intensity. The maximum is centered around $\delta = 1$ kHz, which is consistent with the center of the EIT resonance.

published results [6], but a complete theory, which takes into account the effects of VCCs and finite transit time of the atoms into the beam, gives theoretical results closer to the measured data [10].

For potential applications, the dependence of the group velocity on the Raman detuning is of interest as it can be used for rapidly changing the delay. We recorded delayed pulses for small and controlled pump beam detunings. The pump beam can still be considered as centered in the Doppler profile. If we use again the real part of the susceptibility of Eq. (1), we find that for detunings $\delta \ll \omega_0$, the delay is given by:

$$\tau_g = -\ln(T_0)(2W+\Gamma)\left[\frac{\Omega_C^2}{[2\Gamma_R(2W+\Gamma)+\Omega_C^2]^2+4\delta^2(2W+\Gamma)^2} - \frac{8\delta^2((2W+\Gamma)^2-2\Omega_C^2)\Omega_C^2}{[[2\Gamma_R(2W+\Gamma)+\Omega_C^2]^2+4\delta^2(2W+\Gamma)^2]^2}\right] \tag{5}$$

The dashed curve plotted in Fig. 3 gives the theoretical evolution of τ_g with the averaged intensity if we assume a small 3.8 kHz Raman detuning, as it was visible on the EIT resonances which were recorded the same day. Such a detuning could come from a small residual longitudinal magnetic field. All the other parameters were kept the same as before and chosen to be consistent with our measurements.

Fig. 5 shows the measured evolution of τ_g versus δ, together with the theoretical curve obtained from the above explained model. The values of the parameters were kept as before, except the transmission. It was indeed taken at 35%, which is slightly larger than before, but consistent with the values measured that day. The data were recorded with a very similar but slightly different RF discharge in the helium cell, explaining that difference. One can notice that the curve of Fig. 5 is not centered on $\delta = 0$ kHz but on $\delta = 1$ kHz. This is consistent with the fact that the maximum of the EIT peak recorded at the same time was slightly shifted. This can be explained by a small residual longitudinal magnetic field inside the shielding, which raises the degeneracy between the two Zeeman sublevels. Taking this into account by changing δ into $\delta - \delta_0$ in Eq. (5) with $\delta_0 = 1$ kHz, the theoretical curve is in very good agreement with the experimental points.

4. EIT out of optical resonance: Transition from slow to fast light

The EIT peak transmission is maximum when the Raman detuning between the coupling and the probe beams is zero. It is possible to fulfill this condition with a coupling beam out of optical resonance. However, in this case, EIT resonances are no longer symmetric and exhibit shapes similar to Fano profiles, as explained by Lounis and Cohen-Tannoudji [15]. This cannot be overlooked in Doppler broadened systems, where most atomic velocity classes are out of optical resonance: the recorded resonances are in fact an average of Fano-profiles over all the Doppler width.

If the coupling beam frequency is at the center of the Doppler broadened profile, the recorded resonance is still symmetric because the velocity class optically detuned by a frequency difference $\Delta\nu$ gives a profile symmetric to

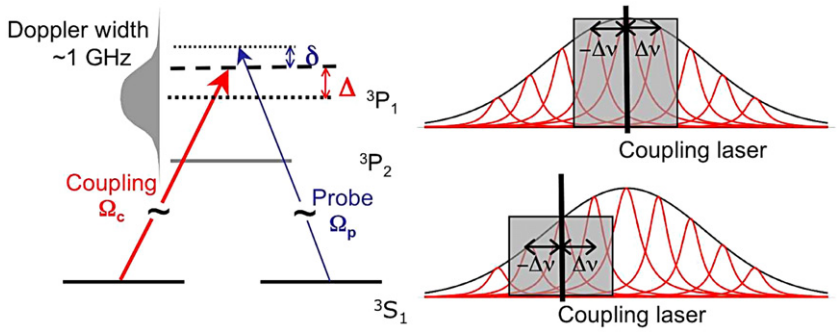

Fig. 6. Notations in a Doppler broadened system. Δ is the coupling beam detuning from the center of the Doppler profile, and δ the Raman detuning between the coupling and probe lasers. On the right, the Gaussian Doppler profile can be divided into Lorentzian sub-profiles corresponding to atomic velocity classes, the transition frequencies of which are Doppler shifted. When the coupling laser frequency is far from the center of the Doppler profile, the optical pumping efficiency is reduced because the velocity classes where it occurs contain less atoms.

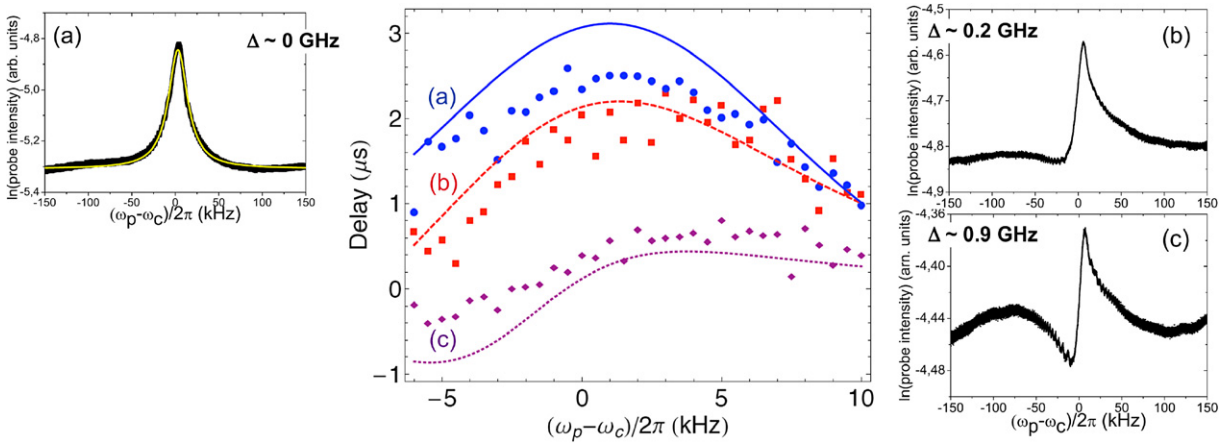

Fig. 7. Measured delays for a 45 W m^{-2} coupling intensity for different optical detunings, corresponding to different initial transmissions: (a) Δ = 0 GHz, $T_0 = 40\%$ (blue circles); (b) 0.2 GHz, $T_0 = 50\%$ (red squares); (c) 0.9 GHz, $T_0 = 70\%$ (purple diamonds). The corresponding theoretical results are respectively plotted as full, dashed, and dotted lines. The side pictures are the corresponding Fano-like profiles, recorded at the same time. (For interpretation of the references to colour in this figure legend, the reader is referred to the web version of this article.)

that given by the velocity class optically detuned by a frequency difference $-\Delta\nu$ (see Fig. 6 for notations). But when the coupling beam is detuned by Δ from the maximum absorption frequency, the numbers of atoms in the velocity classes detuned at $+\Delta\nu$ and $-\Delta\nu$ from the velocity class at resonance with the coupling laser are different. The transmission of these two velocity classes are then different and the weights that they give in the averaging process are not equal. The total absorption is thus asymmetric, as evidenced by the two recorded resonances shown in Figs. 7(b) and 7(c).

A calculation valid at first order in probe beam amplitude, done with the same hypothesis as before, gives the following expression for the susceptibility experienced by the probe beam detuned by $\Delta_P = \omega_P - \omega_0 = \Delta + \delta$:

$$\chi = \frac{Nd^2}{2\epsilon_0\hbar}\left[\frac{4(\delta(\Omega_C^2 - 4\delta\Delta_P) - 4\Gamma_R^2\Delta_P) + 4i(\Gamma_R(2\Gamma_R(2W+\Gamma) + \Omega_C^2) + 2(2W+\Gamma)\delta^2)}{(2\Gamma_R(2W+\Gamma) - 4\delta\Delta_P + \Omega_C^2)^2 + (2\delta(2W+\Gamma) + 4\Gamma_R\Delta_P)^2}\right] \tag{6}$$

The real part of this expression, which is proportional to the logarithm of the transmitted intensity, exhibits an asymmetric shape. Such Fano-like profiles were recorded in helium as reported in Ref. [6]. Fig. 7 shows the shapes of these profiles and the corresponding measured delays for three different values of the detuning Δ of the coupling beam from the center of the Doppler profile. The resonance on the left of the figure is a typical symmetric resonance obtained when the coupling beam is at the center of the Doppler profile. The two asymmetric profiles of Figs. 7(b) and 7(c) were recorded for a coupling detuning Δ around 0.2 and 0.9 GHz, respectively. The profile of Fig. 7(c) displays a clear

transition from slow light ($\tau_g \gg L/c$) to negative group velocity light propagation ($\tau_g < 0$). From the results of Fig. 7, one can see that the light group velocity can be tuned to any value between 10^4 m/s and -5×10^4 m/s. This transition is consistent with the shape of the resonance, the derivative of which changes sign, compared with that in Fig. 7(a). Similar phenomena were already seen some years ago in rubidium vapor by Mikhailov et al. [16] and negative transit times were also experimentally observed in room-temperature gases in the presence of a gain doublet [17]. It should be noticed that superluminal light pulse propagation does not violate causality, if one remembers that the propagation of information is better described by the discontinuities front velocities than by the group velocity [18,19]. A recent experiment in rubidium vapor clearly showed that the superluminal front speed of a Gaussian pulse remains equal to c even with superluminal effect [20].

From Eq. (6), it is possible to determine the theoretical expression of the delay for non-zero optical and Raman detunings:

$$\tau_g = -\ln(T_0)(2W+\Gamma)\left[\frac{\Omega_C^2 - 4\Delta(2\delta + \Gamma_R^2/\omega_0)}{[2\Gamma_R(2W+\Gamma) - 4\delta\Delta + \Omega_C^2]^2 + 4(\delta(2W+\Gamma) + 2\Gamma_R\Delta)^2} - \frac{8((\delta^2\Omega_C^2 - 4\delta\Delta(\delta^2+\Gamma_R^2))((2W+\Gamma)^2 + 4\Delta^2) - 2\delta^2\Omega_C^4 - \Delta\delta\Omega_C^4 + 4\Delta\Omega_C^2(\delta^2+\Gamma_R^2))}{[[2\Gamma_R(2W+\Gamma) - 4\delta\Delta + \Omega_C^2]^2 + 4(\delta(2W+\Gamma) + 2\Gamma_R\Delta)^2]^2}\right] \quad (7)$$

We can see in Fig. 7 that Eq. (7) fits the experimental data quite well. There is a discrepancy for the larger negative Raman detunings when $\Delta = 0.9$ GHz. A possible explanation might be that for such large detunings, the hypothesis of a full optical pumping in the effective width W is not good any more because the coupling beam is already in the wings of the Doppler profile.

5. Conclusion

In conclusion, we have shown that the main features of EIT in a room temperature gas can be simply modeled by introducing an effective linewidth in the usual homogeneous linewidth approach. This has been observed in the case of metastable helium on the EIT window linewidth and peak transmission, together with the delays obtained with zero or non-zero Raman detunings. Moreover, the delays obtained out of optical resonance corresponding to asymmetric Fano-like EIT transmission profiles are also well reproduced by our model. Even further, the negative group velocity effect predicted in the case of strongly optically detuned fields could be observed with our set-up. This optical control of positive and negative group delays opens the way to applications such as adjustable microwave photonics delay lines or controlled nonlinear optics interactions.

Acknowledgements

This work is supported by an Indo–French Networking Project funded by the Department of Science and Technology, Government of India, the French Ministry of Foreign Affairs and also the Indo–French Centre for the Promotion of Advanced Research (IFCPAR/CEFIPRA). The authors are indebted to Hervé Gilles for providing them with some essential parts of the experimental set-up.

References

[1] J.E. Field, K.H. Hahn, S.E. Harris, Observation of electromagnetically induced transparency in collisionally broadened lead vapor, Phys. Rev. Lett. 67 (22) (1991) 3062–3065, doi:10.1103/PhysRevLett.67.3062, http://dx.doi.org/10.1103/PhysRevLett.67.3062.

[2] M.O. Scully, M.S. Zubairy, Quantum Optics, University Press, Cambridge, 1997.

[3] S.E. Harris, J.E. Field, A. Kasapi, Dispersive properties of electromagnetically induced transparency, Phys. Rev. A 46 (1) (1992) R29–R32, doi:10.1103/PhysRevA.46.R29, http://dx.doi.org/10.1103/PhysRevA.46.R29.

[4] L.V. Hau, S.E. Harris, Z. Dutton, C.H. Behroozi, Light speed reduction to 17 metres per second in an ultracold atomic gas, Nature 397 (6720) (1999) 594–598.

[5] M.M. Kash, V.A. Sautenkov, A.S. Zibrov, L. Hollberg, G.R. Welch, M.D. Lukin, Y. Rostovtsev, E.S. Fry, M.O. Scully, Ultraslow group velocity and enhanced nonlinear optical effects in a coherently driven hot atomic gas, Phys. Rev. Lett. 82 (26) (1999) 5229–5232, doi:10.1103/PhysRevLett.82.5229, http://dx.doi.org/10.1103/PhysRevLett.82.5229.

[6] F. Goldfarb, J. Ghosh, M. David, J. Ruggiero, T. Chanelière, J.-L. Le Gouët, H. Gilles, R. Ghosh, F. Bretenaker, Observation of ultra-narrow electromagnetically induced transparency and slow light using purely electronic spins in a hot atomic vapor, Europhys. Lett. 82 (5) (2008) 54002 (6pp.), http://stacks.iop.org/0295-5075/82/54002.

[7] G.V. Shlyapnikov, J.T.M. Walraven, U.M. Rahmanov, M.W. Reynolds, Decay kinetics and Bose condensation in a gas of spin-polarized triplet helium, Phys. Rev. Lett. 73 (24) (1994) 3247–3250, doi:10.1103/PhysRevLett.73.3247, http://dx.doi.org/10.1103/PhysRevLett.73.3247.
[8] A. Robert, O. Sirjean, A. Browaeys, J. Poupard, S. Nowak, D. Boiron, C.I. Westbrook, A. Aspect, A Bose–Einstein condensate of metastable atoms, Science 292 (5516) (2001) 461–464.
[9] F.P. Dos Santos, J. Leonard, J.M. Wang, C.J. Barrelet, F. Perales, E. Rasel, C.S. Unnikrishnan, M. Leduc, C. Cohen-Tannoudji, Bose–Einstein condensation of metastable helium, Phys. Rev. Lett. 86 (16) (2001) 3459–3462.
[10] J. Ghosh, R. Ghosh, F. Goldfarb, J.-L. Le Gouët, F. Bretenaker, Analysis of electromagnetically induced transparency and slow light in a hot vapor of atoms undergoing collisions, Phys. Rev. A 80 (2) (2009) 023817, doi:10.1103/PhysRevA.80.023817, http://dx.doi.org/10.1103/PhysRevA.80.023817, http://link.aps.org/abstract/PRA/v80/e023817.
[11] A. Aspect, E. Arimondo, R. Kaiser, N. Vansteenkiste, C. Cohen-Tannoudji, Laser cooling below the one-photon recoil energy by velocity-selective coherent population trapping, Phys. Rev. Lett. 61 (7) (1988) 826–829, doi:10.1103/PhysRevLett.61.826, http://dx.doi.org/10.1103/PhysRevLett.61.826.
[12] H. Gilles, B. Cheron, O. Emile, F. Bretenaker, A. Le Floch, Rabi–Lorentzian profile of an atomic resonance obtained with Gaussian beams, Phys. Rev. Lett. 86 (7) (2001) 1175–1178, doi:10.1103/PhysRevLett.86.1175, http://dx.doi.org/10.1103/PhysRevLett.86.1175.
[13] E. Courtade, F. Marion, P.-J. Nacher, G. Tastevin, K. Kiersnowski, T. Dohnalik, Magnetic field effects on the 1083 nm atomic line of helium, Eur. Phys. J. D 21 (1) (2002) 25–55, doi:10.1140/epjd/e2002-00176-1, http://dx.doi.org/10.1140/epjd/e2002-00176-1.
[14] E. Figueroa, F. Vewinger, J. Appel, A.I. Lvovsky, Decoherence of electromagnetically induced transparency in atomic vapor, Opt. Lett. 31 (17) (2006) 2625–2627, http://ol.osa.org/abstract.cfm?URI=ol-31-17-2625.
[15] B. Lounis, C. Cohen-Tannoudji, Coherent population trapping and Fano profiles, J. Phys. II 2 (4) (1992) 579–592, doi:10.1051/jp2:1992153, http://dx.doi.org/10.1051/jp2:1992153.
[16] E.E. Mikhailov, V.A. Sautenkov, I. Novikova, G.R. Welch, Large negative and positive delay of optical pulses in coherently prepared dense Rb vapor with buffer gas, Phys. Rev. A 69 (6) (2004) 063808, doi:10.1103/PhysRevA.69.063808, http://dx.doi.org/10.1103/PhysRevA.69.063808.
[17] A. Dogariu, A. Kuzmich, L.J. Wang, Transparent anomalous dispersion and superluminal light-pulse propagation at a negative group velocity, Phys. Rev. A 63 (5) (2001) 053806, doi:10.1103/PhysRevA.63.053806, http://dx.doi.org/10.1103/PhysRevA.63.053806.
[18] J.C. Garrison, M.W. Mitchell, R.Y. Chiao, E.L. Bolda, Superluminal signals: Causal loop paradoxes revisited, Phys. Lett. A 245 (1–2) (1998) 19–25, doi:10.1016/S0375-9601(98)00381-8, http://dx.doi.org/10.1016/S0375-9601(98)00381-8.
[19] M.D. Stenner, D.J. Gauthier, M.A. Neifeld, Fast causal information transmission in a medium with a slow group velocity, Phys. Rev. Lett. 94 (5) (2005) 053902, doi:10.1103/PhysRevLett.94.053902, http://dx.doi.org/10.1103/PhysRevLett.94.053902.
[20] H. He, Z. Hu, Y. Wang, L. Wang, S. Zhu, Superluminal light propagation assisted by Zeeman coherence, Opt. Lett. 31 (16) (2006) 2486–2488, http://ol.osa.org/abstract.cfm?URI=ol-31-16-2486.